EFFECT OF Si ANTIOXIDANT ON THE RATE OF OXIDATION OF CARBON IN MgO–C REFRACTORY

S.K. Sadrnezhaad*

Center of Excellence for Production of Advanced Materials, Department of Materials Science and Engineering
Sharif University of Technology, P.O. Box 11365-9466, Tehran, Iran
sadrnezh@sharif.edu

N. Bagheri

Materials and Energy Research Center, P.O. Box 14155-4777, Tehran, Iran
nbs1384@yahoo.com

S. Mahshid

Center of Excellence for Production of Advanced Materials, Department of Materials Science and Engineering
Sharif University of Technology, P.O. Box 11365-9466, Tehran, Iran
sara_mahshid@yahoo.com

*Corresponding Author

(Received: January 08, 2010 – Accepted in Revised Form: October 20, 2011)

doi: *10.5829/idosi.ije.2011.24.04b.06*

Abstract Progressive conversion/shrinking core (PC-SC) models of constant-size cylinders were exploited to interpret the decarburization reactions of MgO-C-Si bricks heated up under blown air. Chemical adsorption/solid (or pore) diffusion mechanisms governed the reaction rate. With 5% silicon, chemical adsorption vanished at 1000 and 1100°C. The oxidation rate lowered then with temperature. This was due apparently to the blocking of the pore-end gorges by the voluminous compounds (like Forstrite). Arrhenius plots of the specific rates yielded the activation energies of the prevailing steps. Without Si antioxidant, three steps were appreciated having activation energies of 51.65 (for chemical adsorption), 125.75 (for solid-phase diffusion) and 9.08 KJ/mol (for pore diffusion). With 5 wt% silicon addition, two steps existed with activation energies of 51.65 (for chemical adsorption) and 134.59 KJ/mol (for solid-phase diffusion). These values were slightly lower than the corresponding activation energies reported earlier for MgO-C and MgO-C-Al systems. Small differences could apparently attribute to the tortuosity differences of the samples.

Keywords Refractory, MgO–C, Silicon, Antioxidant, Kinetics, Oxidation, PC-SC

چکیده در این تحقیق، از دو مدل تبدیل فزاینده و هسته کوچک شونده برای تفسیر نتایج تجربی حاصل از کاهش محتوای کربن در اثر حرارت دهی آجر استوانه‌ای شکل منیزیا-گرافیت-سیلیسیوم دارای قطر ثابت در مجاورت هوا استفاده شد. معلوم شد که مکانیزم کنترل کننده سرعت، جذب شیمیایی همراه با نفوذ در جامد (یا در حفره تخلخل) است. در نمونه دارای ۵% سیلیسیوم، در حالی که جذب شیمیایی در دماهای ۱۰۰۰ و ۱۱۰۰ درجه سانتیگراد نقش کنترلی خود را از دست می‌داد، سرعت اکسیداسیون هم در عین حال کاهش می‌یافت. این کاهش ظاهرا" به سبب مسدود شدن حفره‌ها به وسیله ترکیبات نسبتا" پر حجم حاوی سیلیسیوم مانند فورستریت بود. با استفاده از معادله آرنیوس، انرژی‌های تحریک مراحل اثر گذار بدین قرار تعیین شد: بدون سیلیسیوم، سه مرحله با انرژی‌های تحریک به ترتیب ۵۱/۶۵ (برای جذب شیمیایی)، ۱۲۵/۷۵ (برای نفوذ در فاز جامد) و ۹/۰۸ کیلوژول بر مول (برای نفوذ در حفرات تخلخل) وجود دارد. با ۵% سیلیسیوم، فقط دو مرحله با انرژی‌های تحریک به ترتیب ۵۱/۶۵ (برای جذب شیمیایی) و ۱۳۴/۵۹ کیلوژول بر مول (برای نفوذ در فاز جامد) موجود است. این ارقام اندکی کوچکتر از مقادیر گزارش شده قبلی برای اکسید شدن دیرگدازهای منگنزیا – گرافیت و منگنزیا – گرافیت – آلومینیوم است که شباهت اثر دو ماده انتی اکسیدان را تا حد زیادی آشکار می‌سازد. علت تفاوت مقادیر انرژی تحریک، بنابراین می‌تواند به تفاوت پیچ در پیچی حفره‌های تخلخل در دیرگدازهای مشابه دارای سیلیسیوم و آلومینیوم مربوط باشد

1. INTRODUCTION

MgO-C refractories are widely used in the melt shops on the account of their distinct resistance to thermal shock, lessened thermal expansion, admissible corrosion resistance and low wettability with corrosive slags [1- 4]. High temperature oxidations cause, however, a dramatic property alteration due to graphite diminution [1, 2, 5]. Once the graphite is dismissed, the material becomes susceptible to slag corrosion and thermal shock [6, 7]. The oxidation reactions (direct or indirect) have been the subject of numerous investigations [8-15].

To overcome the graphite oxidation, various antioxidants are added to the burden batches used for brick fabrication [2, 5]. The antioxidants often used in MgO-C refractories include metals (such as Al, Si and Mg) and alloys (such as Al-Mg and ferrosilicon), carbides (such as B_4C and SiC) and borides (such as SiB_6 and ZrB2) [5, 7, 16, 17].

Reactions of silicon, graphite and the atmospheric gases result in formation of different compounds like SiC, Si_3N_4, SiO_2 and Mg_2SiO_4 which affect behavior of the MgO-C bricks. Previous researchers have studied some of these reactions taking place in the MgO-C bricks containing Si and/or SiC antioxidants [5, 16, 18]. Standard free energies of typical reactions evaluated in joules per mole are as follows [16, 19, 20]:

$$Si(s) + C(s) \rightarrow SiC(s)$$
$$\Delta G^o = -53943 + 7.29T \qquad 298<T<1686K \quad (1)$$

$$Si(s) + O_2(g) \rightarrow SiO2(s)$$
$$\Delta G^o = -902070 + 173.64T \qquad 700<T<1700K \quad (2)$$

$$3Si(s) + 2N_2(g) \rightarrow Si_3N_4(s)$$
$$\Delta G^o = -731118 + 320.31T \qquad 298<T<1686K \quad (3)$$

$$3SiC(s) + 2N_2(g) \rightarrow Si_3N_4(s) + 3C(s)$$
$$\Delta G^o = -569289.00 + 298.44T \qquad 298<T<1686K \quad (4)$$

$$SiC(s) + 2CO(g) \rightarrow SiO2(s) + 3C(s)$$
$$\Delta G^o = -732587 + 356.23T \qquad 700<T<1700K \quad (5)$$

$$SiO_2(s) + 2MgO(s) \rightarrow Mg_2SiO_4(s)$$
$$\Delta G^o = -67200 + 4.31T \qquad 298<T<1700K \quad (6)$$

Ample studies have been carried out regarding the influence of antioxidants on mechanical and micro-structural properties of MgO-C bricks [5, 21- 28]. However, there are still scarce resources on the oxidation mechanisms of these refractories in presence of single and multi antioxidants commercially used in refractory production industries [13-15].

Wang et al [29] have studied the effect of $Al_8B_4C_7$ antioxidant on the oxidation behavior of MgO-C refractory. They mentioned the reaction of $Al_8B4C_7(s)$ with CO (g) to form $Al_2O_3(s)$, B_2O_3 (l) and C(s) at temperatures greater than 1100°C. The Al_2O_3 produced reacts with MgO to form $MgAl_2O_4$ near the surface of the solid sample. $B_2O_3(l)$ evaporates concomitantly, and then reacts with MgO to form a liquid phase at temperatures above 1333°C (the eutectic point between $3MgO.B_2O_3$ and MgO). The coexistence of the liquid phase and $MgAl_2O_4$ makes the protective layer denser and inhibits further oxidation of the refractory materials. At temperatures greater than 1333°C, the oxidation is apparently controlled by oxygen diffusion. At temperatures lower than 1333°C, the chemical reaction prevails [29].

Yamaguchi [30] has shown that the aluminum vapor diffuses through the refractory materials reacting with the carbon and N_2 to form $Al_4C_3(s)$ and AlN(s) whiskers, respectively. These processes plus the reactions proceeding to the formation of $MgO.Al_2O_3(s)$ spinel result in great morphological changes which reduce the refractory oxidation-rate [16].

Kinetics of air-oxidation of MgO–C–Al refractory at 600–1300°C has been investigated by Sadrnezhaad et al [2]. Addition of aluminum antioxidant indicated a reducing effect on oxidation of MgO–C bricks at $800 \leq T \leq 1250$°C. Reverse behavior has been observed at $T \leq 700$°C. Further studies have been carried out on the oxidation kinetics of MgO-C bricks by Carniglia [31], Tabata et al [32], Ichikawa et al [36], Ghosh et al [8], Faghihi-Sani et al [9] and Xiangmin et al [10]. These investigators have shed some light on the oxidation kinetics of the graphite in the MgO-C system. For example, the overall activation energy of air oxidation of the MgO–C-Al brick hasbeen found to be 139.15 kJ/mol at $T \leq 800$°C (for internal diffusion) and 25.48 kJ/mol at $T > 800$°C (for pore diffusion) [2]. The corresponding values

for MgO–C oxidation reactions have been [2]: (a) 134.85 KJ/mol (for internal diffusion) and 66.69 KJ/mol (for chemical adsorption) at T≤ 800°C and (b) 18.95 kJ/mol (for pore diffusion), and 66.69 kJ/mol (for chemical adsorption) at T> 800°C. Mechanisms of oxidation of MgO–C refractories in presence of other antioxidants like silicon are not so clearly known.

This paper focuses on the kinetics of air oxidation of MgO-C refractory in presence of Si antioxidant at temperatures between 600 and 1250°C. The experimental procedure is similar to that described earlier [1, 2]. Progressive conversion/ shrinking core models of constant size cylindrical shape particles are used to interpret the empirical data obtained during this research [31, 32]. Based on the mechanisms suggested, the total conversion times and the activation energies of the processes are analytically evaluated.

2. EXPERIMENTAL PROCEDURE

The MgO-C-Si bricks were made of the raw materials by (a) weighting according to the compositional ratios given in Table 1, (b) dry-mixing in a steel container, (c) cold pressing into cylindrical molds having 300mm diameter and 20mm height, and (d) heating at 600°C for 7 hours in a coke bed for its volatile matters to exhaust. Size distribution and percent substances mixed to make samples S0, S1, S3 and S5 (containing 0, 1, 3 and 5 wt % silicon, respectively) are summarized in Table 1. Apparent density and porosity of the samples were measured by oil before and after the heating process, according to ASTM standard. The results are given in Table 2.

It is seen that both bulk and apparent densities of the probes diminish with silicon content (see Table 2). This seems due to the lower density of silicon as compared to that of magnesium oxide. A meaningful change in the apparent porosity is not, however, observed with the silicon content. This may be due to the similar grain distribution of the two commercially made systems.

TABLE 1. Composition of MgO-C Refractory Bricks

Material / Sample Number		S0	S1	S3	S5
Fused MgO, China	3-5 mm (%)	19	19	19	19
	1-3 mm (%)	28	28	28	28
	0.075-1 mm (%)	28	28	28	28
Sintered MgO <0.075 mm (%)		15	14	12	10
Flake Graphite, China (%)		10	10	10	10
Si Powder <0.075 mm (%)		0	1	3	5
Phenolic Resin (%)		3	3	3	3

Oxidation tests were carried out in an isothermal tube furnace at 600, 700, 800, 900, 1000 and 1100°C, while air was purged into the furnace from two nozzles located at the bottom of the furnace. After the furnace reached to a predetermined temperature, the sample was moved to the hot zone of the furnace by a fused silica holder leaned on a digital balance indicating the total weight of the sample plus the holder. The experimental set up is shown in Figure 1. In order to provide a unidirectional oxidation process, the top and bottom bases of the cylindrical sample were covered by two alumina plates to prevent contact with air. Weight changes of the samples were recorded against time for around 2 hours. The fractional conversion X was assumed to be equal to the weight loss fraction of the samples being calculated from the following equation:

$$X = \frac{\text{Weight Loss}}{\text{Total Weight Loss After Complete Oxidation at 1100 }^{o}\text{C}} \quad (7)$$

TABLE 2. Results of the Archimedes Test for Refractory Brick Samples

Sample	S0		S1		S3		S5	
	Raw Brick	After Curing	Raw Brick	After Curing	Raw Brick	After Curing	Raw Brick	After Curing
Bulk Density (Kg/m^3)	2990	2970	2960	2930	2930	2900	2870	2850
Apparent Density (Kg/m^3)	3190	3240	3160	3210	3130	3200	3130	3160
Apparent Porosity (%)	7.37	8.55	6.90	9.71	7.38	8.98	8.21	9.64

In order to determine the total weight loss, the samples were completely oxidized at 1000°C in a box furnace. X-ray diffraction (XRD) patterns of the samples were determined by Philips PW 3710 X-Ray diffractometer using CuKα radiation (λ=1.5405Å).

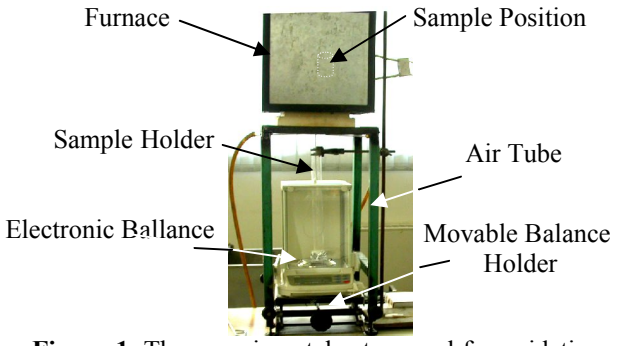

Figure 1. The experimental setup used for oxidation weight–loss measurements of the MgO-C-Si bricks

3. RESULTS AND DISCUSSION

Figure 2 shows the images of the different areas of the sample S0 taken by an optical-microscope. The shiny part is related to the graphite rich core (Figure 2a). The reacted/unreacted interface is shown both schematically and by micro-photography in Figure 2b. Other surfaces relate to the reacted ash shell (Figure 2c).

Photographs of the cross-sections of the specimen S5 partially oxidized at (a) 900, (b) 1000 and (c) 1100°C are shown in Figure 3. The central dark areas correspond to the graphite rich cores of the probes surrounded by the ash shells totally depleted of any remained graphite content during the oxidation which starts from exterior and progresses towards the core.

Optical-microscope images of the cross section of the sample indicate that the graphite flakes do not bend during pressing of the raw mixture to

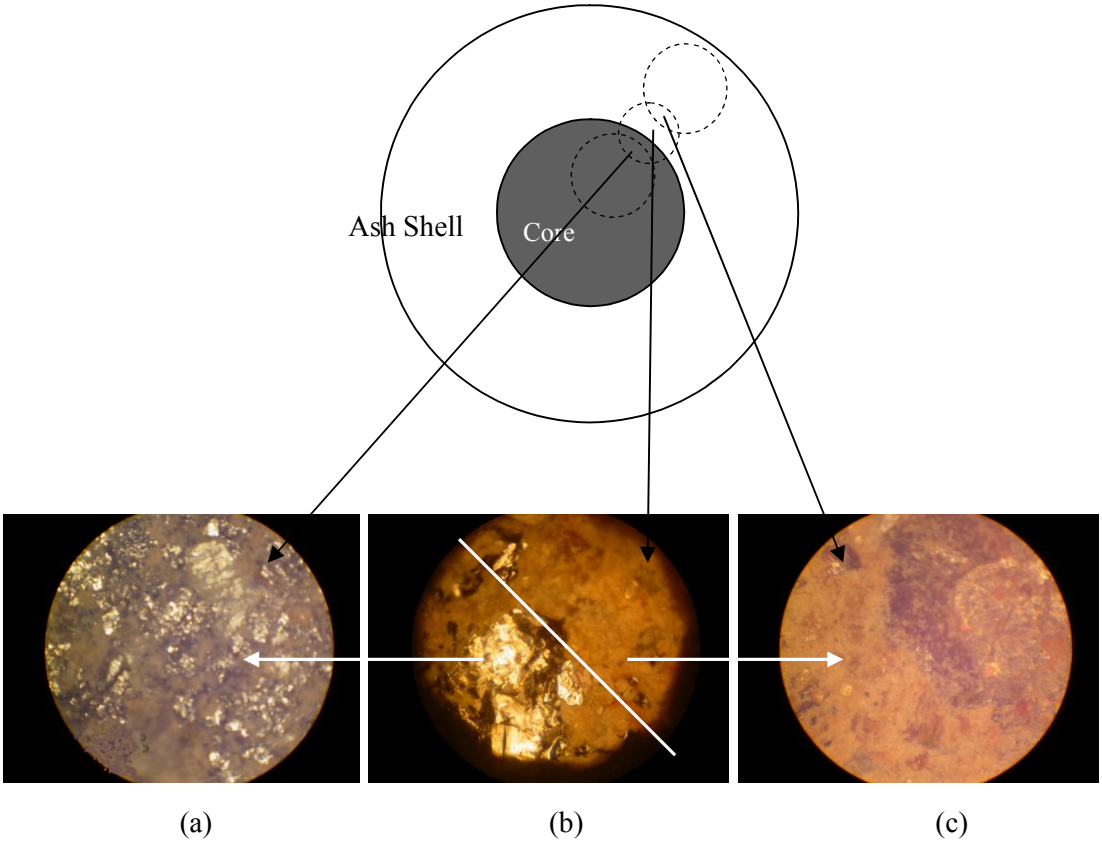

Figure 2. Optical microscope images of the sample S0: (a) unreacted core with shiny planes showing graphite rich regions (×40), (b) the reacted/unreacted interface (×100) and (c) the reacted (ash) shell (×40).

make refractory brick specimens. They maintain their initial planar shape that may even split up under heavy pressure (Figure 4).

(a) (b) (c)

Figure 3. Sample S5 oxidized for 150 minutes at (a) 900°C, (b) 1000°C and (c) 1100°C.

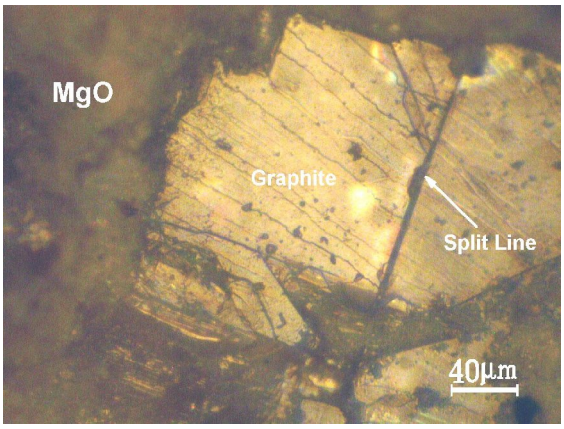

Figure 4. Optical-microscope image of a large graphite flake seen on the cross section of the S0 sample. The initial flake size is around 420×480 µm

Meticulous observations indicate no dimensional-change of the probe during oxidation in the MgO-C-Si samples. PCSC models developed for constant-size particles can thus be used to interpret the oxidation processes [1, 2, 33-35]. These models are devised based on the assumption that several serial and/or parallel steps can control the rate of reactions both individually or cooperatively:

(a) Gas transfer to the surface of the sample (ED),

(b) Gas transfer through the porous regions of the sample (ash) towards the reactive sites (PD),

(c) Internal diffusion of the oxidizing/reducing gases through the solid phases surrounding the graphite flakes (ID),

(d) Chemical adsorption of the gases onto the surface of the graphite flakes (CA), and

(e) Reaction of the graphite flakes with oxygen (CR).

Both models relate the oxidation time of samples to their total conversion times by combining mass conservation with chemical rate-equations to obtain:

$$t = \tau_{ED} f_{ED}(X) + \tau_{PD} f_{PD}(X) + \tau_{ID} f_{ID}(X) + \tau_{CA} f_{CA}(X) + \tau_{CR} f_{CR}(X) \quad (8)$$

For the specific cylindrical geometry of the sample, the dimensionless functions fij(X) can be defined as follows [1, 2]:

(a) Unidirectional gas transfer outside the cylinder $f_{ED}(X) = X$

(b) Pore inter-diffusion of the gases $f_{PD}(X) = X + (1-X)\ln(1-X)$

(c) Internal diffusion of oxygen towards the flat graphite flakes $f_{ID}(X) = X^2$

(d) Adsorption/desorption of the gases onto the surface of the flat graphite flakes $f_{CA}(X) = X$

(e) Graphite oxidation reactions $f_{CR}(X) = X$

Sadrnezhaad et al [1, 2] have reported that the alteration from internal to pore diffusion mechanism occurs at around 800°C. This is due to the very limited number of open pores bellow 800°C and their relative increase above that temperature. Appropriate mechanisms can be found by comparing the experimental data with the mathematical correlations. The KDA software reported by Sadrnezhaad et al [1, 12] can help the dreary lengthy calculations.

Results of the model calculations are summarized in Table 3. From previous investigations [1, 2], it is known that the rate of chemical reaction is fast enough not to be considered as a limiting step. The alteration temperature of the mechanism can, thus, be found by plotting the ratio of $\tau_{ID \text{ or } PD}$ to τ_{CA} (Figure 5) versus temperature. Accordingly, the alteration temperature for mechanism of the oxidation is around 800°C. This result is fairly consistent with those obtained for MgO-C [1] and MgO-C-Al [2] oxidation, before. According to Figure 5, addition of silicon does not significantly change the alteration temperature.

Adsorption control is due to the small surface energy of graphite flakes and their relatively low speed of bonding with atmosphere. This has also been reported by previous researchers for samples without antioxidant [2]. This effect is, however, weakened with increasing temperature (Table 3) and totally vanishes in the samples containing 5% silicon (sample S5) at 1000 and 1100°C (Table 3).

Sadrnezhaad et al [2] have reported that the addition of aluminum results in the formation of metal-oxygen bonds which breaks the O-O bonds. Weakening of the π bonds of C atoms facilitates the oxygen chemisorption [37]. Aluminum seems, therefore, to have a catalytic effect and to increase the chemisorption rate of oxygen to the surface of the graphite flakes [38]. The expedition of the chemical adsorption seems to signify the diffusion controlling effect, so much that it converts into a sole rate-determining step when the aluminum antioxidant is present in the sample. According to previous investigations, the interfacial interaction of aluminum and its compounds with graphite totally eliminates the chemisorption step from the oxidation mechanism of the MgO–C–Al brick [2]. Comparing the experimental data of this investigation with MgO-C-Al system indicates that although silicon plays a similar catalytic role at higher temperatures (1000 and 1100°C), low temperature behavior is weaker than the latter (Table 3). The silicon content needs, for example, to be at least 5% for total elimination of the adsorption controlling effect at 1000 and 1100°C.

The catalytic effect of silicon in different media has been reported by previous investigators [38,39]. The reason for the lower silicon effect rests on its smaller vapor pressure compared to that of aluminum which causes greater catalytic effect. Figure 6 compares the vapor pressures of the two antioxidants versus temperature. For a similar vapor pressure, a higher temperature is required to expect a comparable behavior [40].

As it can be seen from the weight-loss curves (Figures 7 and 8), for samples S3 and S5, the weight loss rate at 1100°C becomes less than that at 1000°C. It also can be seen from Figure 3 (b and c) that the surface area of the unreacted core of the sample heated at 1000°C is smaller than that of the sample heated at 1100°C. This is due to the

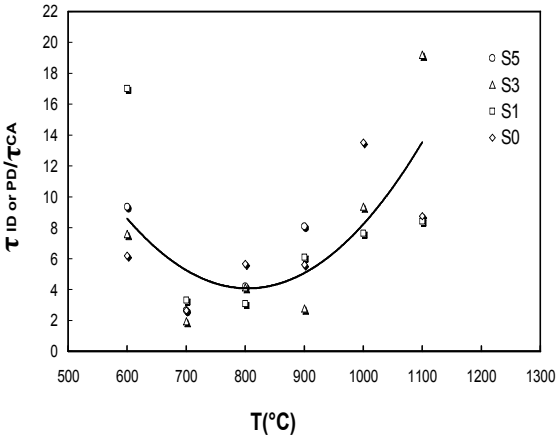

Figure 5. Variation of the $\tau_{ID\ or\ PD}/\tau_{CA}$ ratio versus the oxidation temperature for S0, S1, S3 and S5 samples.

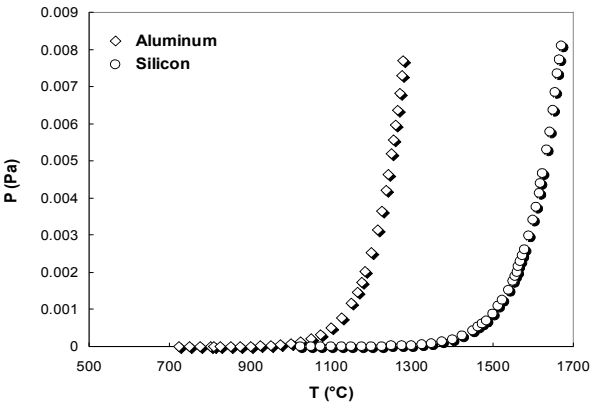

Figure 6. Vapor pressure versus temperature for Silicon and Aluminum [40]

TABLE 3. Total Conversion Times of the Samples S0, S1, S3 and S5 at Different Temperatures.

T(°C)	$\tau_{ID\ or\ PD(ks)}$				$\tau_{CA(ks)}$			
	S0	S1	S3	S5	S0	S1	S3	S5
600	2169.31	2625.98	1713.90	3261.80	350.20	154.36	225.54	348.41
700	365.59	454.70	469.04	485.09	138.70	137.18	241.68	182.39
800	438.54	274.98	331.96	297.58	77.59	89.20	80.13	70.68
900	272.13	318.75	354.76	348.86	48.51	52.34	128.00	43.12
1000	271.39	285.55	274.53	487.17	20.08	37.35	29.34	-
1100	309.77	312.44	688.01	1025.53	35.4	37.08	35.82	-

presence of a high amount of Si in these samples and the formation of highly expanding silicon carbide and Forstrite phases [16, 17]. Solid material expansion closes the pores and prevents the diffusion of oxygen by excessive core shrinkage which reduces the oxidation rate. Solid-phase diffusion will then become the prevailing kinetic step. This is of course much slower than the pore diffusion.

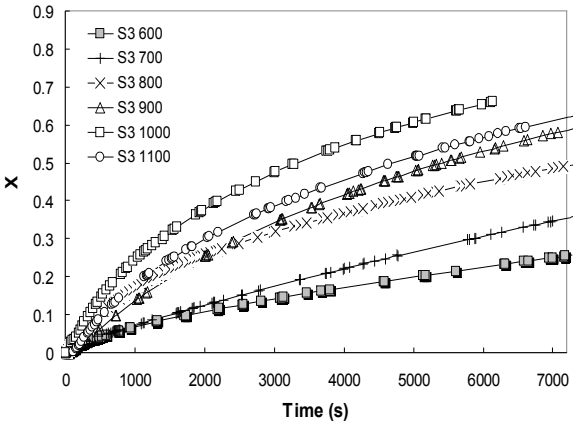

Figure 7. Weight loss versus time for S3.

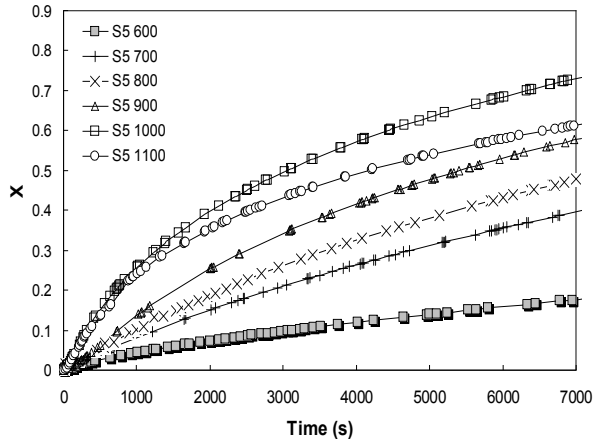

Figure 8. Weight loss versus time for S5.

Figure 9 illustrates XRD patterns of the refractory samples before and after oxidation with different Si contents. According to the previous researches, the Forstrite formation occurs at higher temperatures (1200°C and higher) [41, 42]. Its formation is, however, thermodynamically feasible even at slightly lower (1100°C) temperatures [43]. With small amount of silicon used in this research (3 and wt 5%) and the overlap between different X-ray diffraction peaks of the samples, the quantities of the phases are so small that their presence is hardly assessable on X-ray patterns (Figure 9).

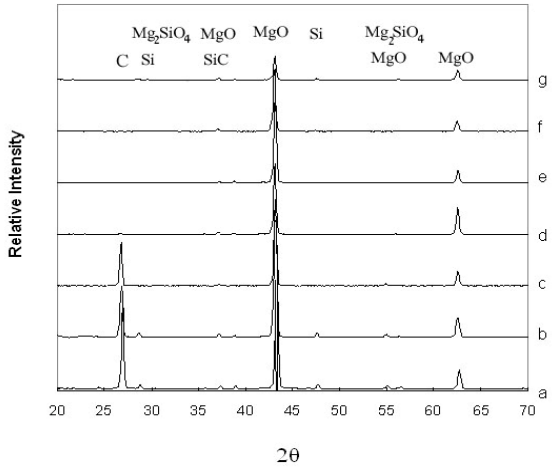

Figure 9. X-ray diffraction patterns of (a) S5, before oxidation, (b) S5, after oxidation at 600°C, (c) S0, reacted shell after oxidation at 1100°C, (d) S0, unreacted core after oxidation at 1100°C (e) S1, reacted shell after oxidation at 1100°C, (f) S3, reacted shell after oxidation at 1100°C, (g) S5, reacted shell after oxidation at 1100°C.

Several researchers have elaborated on this matter. Ahmadi, et al [41] have, for example, reported the formation of expanding phases at 1300°C. Ghosh, et al [42] have reported the formation of SiC at 1200°C. Smith [43] has indicated the probable formation of this phase at 1000 to 2000°K. At 1200°C, silicon reacts with carbon monoxide to form silicon carbide. SiC can also react with CO to firstly form SiO, and secondly SiO_2 and with MgO to form Forsterite (Mg_2SiO_4) [42]. The most probable thermodynamic path followed for formation of these phases may thus be that of the reactions summarized in Equations 1 to 6 [18-20].

According to the previous researchers, three other reactions are also plausible resulting in the formation of Forstrite which result in the volume expansion in solid particles of the system [41, 42]. These reactions can be summarized as:

In the edges of the Magnesia particles

$$2MgO_{(S)}+SiO_{(g)}+CO_{(g)} \longrightarrow Mg_2SiO_{4(S)}+C_{(s)}$$

$700<T<1700K \quad \Delta G^{o}=-860033.10-343.8T$

Inside the sample

$2Mg_{(g)}+SiO_{(g)}+3CO_{(g)} \longrightarrow Mg_2SiO_{4(s)}+3C_{(s)}$

$700<T<1700$ $\Delta G^o=2045639.4-61.68\ T\ logT+1152.55T$

In the vicinity of the sample surface

$Mg_{(g)}+1/2O_2 \longrightarrow MgO_{(s)}$

$1380<T<2500$ $\Delta G^o= -759814-30.84\ T\ logT+316.73T$

Shouxin, et al [44] have reported that Si particles form a coating layer of SiO_2 around themselves. Covered Si can only oxidize when the coating layer is removed. Another probability is the reaction of SiO_2 with carbon to form the gaseous SiO [21-23]. Zhang [16] believes that when SiC is exposed to CO, SiO(g) will be formed. SiO will then react with MgO to form Forstrite in the reductive atmosphere around the core, and at the same time will diffuse towards the exterior hot surface of the refractory brick to be oxidized into SiO_2.

In order to prove the solid phase expanding behavior of silicon, partially oxidized S0 and S5 samples were both immersed into an inky aqueous solution. After some time the samples were taken out and sliced off their cross-section. The ink diffusion depth in the S0 was much greater than that in the S5 indicating the presence of much higher open pores in the probe without antioxidant (Figure 10).

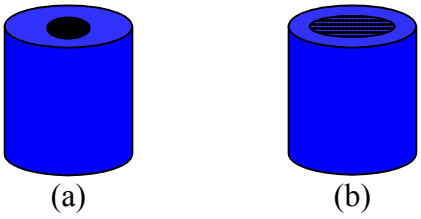

Figure 10. Schematic of the ink diffusion in samples partially oxidized at 1100°C: (a) S0 and (b) S5 probe

The activation energies of different oxidation steps were determined by applying Arrhenius theorem to results of the model calculations. Plots of ln $(1/\tau_{CA})$, ln $(1/\tau_{ID})$ or ln $(1/\tau_{PD})$were drawn versus 1/T and their slopes were multiplied by –8.314j/mol to determine the values for activation energy. The results are given in Table 4.

Sadrnezhaad, et al [1] have previously reported Q_{CA}= 62.54, Q_{ID}= 134.86 and Q_{PD}= 19.11 kJ/mol for samples without antioxidant and Q_{ID} = 139.16 and Q_{PD} = 25.5 kJ/mol for the samples containing 1.5%Al [2]. These values are slightly greater than the activation energies obtained with and without silicon content in this research. The inter-diffusion of the gases in the refractory pores depends on tortuosity and shape factor of the pores. Large open-ended pores can facilitate passage of the gases and indicate greater diffusion coefficient with lower activation energy. When proportion of the medium size grains are higher (Figure 11, data of this research), a relatively uniform distribution can produce lower tortuosity with higher porosity which may cause lower pore-diffusion effect observed in this research. With close ended tortuous pores, solid diffusion should help the passage of gases to the reaction sites for continuation of oxidation reactions. The activation energy for the latter is generally much higher than that of the pore diffusion process.

As it can be seen from the activation energy data of Table 4, Si and Al behave the same way when a small amount of these metals are added to the refractory sample. But the trend may be

TABLE 4. Activation Energies of chemisorption, solid diffusion and pore diffusion for air oxidation of MgO-C and MgO-C-Si Samples.

Sample	S0	S1	S3	S5
Q_{CA}(kJ)	51.65	32.88	42.16	51.65
Q_{ID}(kJ)	125.75	123.84	91.51	134.59
Q_{PD}(kJ)	9.08	8.8	-	-

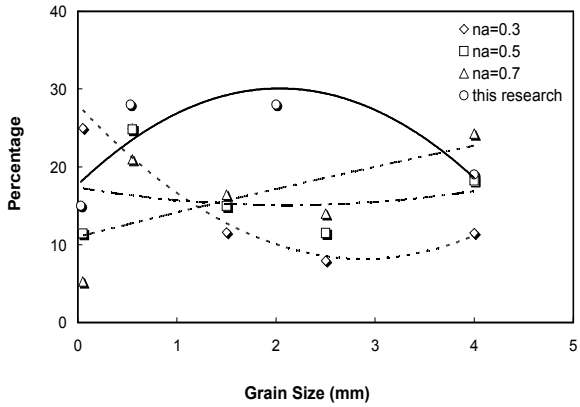

Figure 11. A comparison of MgO grain size used in this research with that used in previous researches [1, 2] for different Andreasen numbers of n_a= 0.3, 0.5 and 0.7

changed at higher contents. According to some researchers [45-47], the high hydration capability of Al_4C_3 produced by the carbon and aluminum reaction would, for example, result in a change in the governing mechanism. This phase will intensely be hydrated and the resulting aluminum hydroxide will cause a high volume expansion which will result in the formation of cracks and sometimes the collapse of the brick strength. The higher the amount of Al antioxidant, the higher would be the risk of hydration. This phenomenon has not been reported for the samples containing high Si antioxidants.

4. CONCLUSIONS

1. Oxidation of the refractories with and without up to 5 wt% Si antioxidant is controlled by a two-step solid-phase diffusion/chemical adsorption process at temperatures lower than 700°C and by a two-step pore-diffusion/chemical adsorption process at temperatures higher than 700°C.
2. With 5 wt% Si content, the chemical adsorption mechanism is removed at 1000 and 1100°C due to the Si catalyzing effect.
3. The experimental results obtained for the refractories without antioxidant and with 1% Si were comparable with those having similar Al additions. In the case of 3 wt% and 5 wt% Si antioxidant, due to the volume expansions resulting from the formation of silicon containing phases, the open porosities were decreased which caused the lowering of gas phase diffusion into the porous probe. Hence, the oxidation rate of the refractory sample decreased by incresing temperature from 1000 to 1100°C.
4. The presence of Si and its relative reactions seems to cause a large deviation from the mechanisms based on the air/carbon reactions.

5. REFERENCES

1. Sadrnezhaad, S.K., Mahshid, S. Hashemi, B. and Nemati, Z.A., "Oxidation Mechanism of C in MgO–C Refractory Bricks", ***Journal of the American Ceramic Society***, Vol. 89, No. 4, (2006), 1308-1316.
2. Sadrnezhaad, S.K., Nemati, Z.A., Mahshid, S., Hosseini S. and Hashemi, B., "Effect of Al Antioxidant on the Rate of Oxidation of Carbon in MgO–C Refractory", ***Journal of the American Ceramic Society***, Vol. 90, No. 2, (2007), 509-515.
3. Banerjee, S., "Recent Developments in Steel-making Refractories", ***Unitecr 01, Proceedings 91***, Mexico (2001), 1033–1041.
4. Rigaud M. and Ningsheng, Z., "Major Trends in Refractories Industry at Beginning of the 21st Century", ***China's Refractories***, Vol. 11, No. 2, (2002).
5. Nemati, Z., Sadrnezhaad, S., and Mooghari, H.R.A., "Effect of Ferrosilicon, Silicon and Aluminum Antioxidants on Microstructure and Mechanical Properties of Magnesia–Graphite Refractory", ***Refractories Applications & News***. Vol. 10, No. 6, (2005), 17-23.
6. Sereno E. and Brosnan, D.A., "Effect of Organic Fiber Additions on the Mechanical Properties of MgO–C Bricks", ***Proceedings of the Unified International Technical Conference on Refractories***, New Orleans, LA, (1997), 775–82.
7. Sarkkinen R.J. and Harkki, J.J., "Thermodynamic Calculation of Reactions Inside MgO-C Antioxidant Linings", ***Unified International Technical Conference on Refractories, Finland***, (1997), 755–63.
8. Ghosh, N., Ghosh, D., and Jagannathan, K. "Oxidation Mechanism of MgO-C in Air at Various Temperatures", ***British ceramic transactions***. Vol. 99, No. 3: (2000), 124-128.
9. Faghihi-Sani, M.A. and Yamagyshi, A., "Oxidation Kinetics of MgO-C Refractory Bricks", Ceramic International, Vol. 28, (2002), 835-839.
10. Xiangmin Li, Michel Rigaud and Stefan Palco, "Oxidation Kinetics of Graphite Phase in MgO-C Refractories", ***Journal of the American Ceramic Society***, Vol. 78, No. 4, (1995), 965-971.
11. Hashemi, B., Nemati, Z.A. and Sadrnezhaad, S.K., "Oxidation Mechanisms in MgO-C Refractories", China Refractories, Vol. 13, No. 2, (2004), 13-20.
12. Hashemi, B., Moghimi, Z., Nemati, Z.A. and Sadrnezhaad, S.K., "Solid-Gas reactions in MgO-C Refractories", ***4th ISARIM-Symposium on Refractories, MET Society, Hamilton- Canada***, (2004), 581-91.
13. Zheng, H-Z; Liang, Y-H; Wu, Y-Y; Qiu, W-D, "Influence of Antioxidant on the Oxidation Resistance of Regenerate Al(2)O(3)-MgO-C Bricks", ***Journal of Wuhan University of Science and Technology (Natural Science Edition),*** Vol. 26, No. 1, (2003) 11-13.
14. Takeuchi, K; Yoshida, S; Tsuboi, S, "Gas Phase Oxidation of MgO-C Bricks", ***Refractories*** (Tokyo), Vol. 55, No. 3, (2003), 128-131.
15. Tsuboi, S., Yoshida, S., and Takeuchi, K., "Gas Phase Oxidation of MgO-C Bricks", ***Journal of Technology Associaton Refractories Japan***. Vol. 22, No. 3: (2002), 270.
16. Zhang, S., Marriott, N., and Lee, W., "Thermochemistry and microstructures of MgO-C refractories containing various antioxidants", ***Journal of the European Ceramic Society***. Vol. 21, No. 8: (2001), 1037-1047.
17. Zhang S. and Lee, W.E., "Influence of Additives on Corrosion Resistance and Corroded Microstructures of

MgO–C Refractories", J. Eur. Ceram. Soc., 21 [13] 2393-2405 (2001).
18. Uchida S. and Ichikawa, K., ‘‘High Temperature Properties of Unburned MgO–C Brick Containing Al and Si Powders", ***Journal of the American Ceramic Society***, Vol. 81, No. 11, (1998), 2910–2916.
19. Sadrnezhaad, S.K., "Heat and Motion in Materials", Foreign Ministry Press, Tehran, Iran, (1999). (ISBN 964-330-526-X).
20. Gaskell, D.R., "*Introduction to the Thermodynamics of Materials"*. Hemisphere Pub (2003).
21. De la Torre, Ã.G., Valle, F.J., and De Aza, A.H., "Direct mineralogical composition of a MgO-C refractory material obtained by Rietveld methodology", ***Journal of the European Ceramic Society***. Vol. 26, No. 13: (2006), 2587-2592.
22. Baudin, C. Alvarez C. and Moore, R.E., "Influence of Chemical Reaction in Magnesia–Graphite Refractories: II- Effects of Aluminum and Graphite Content in Generic Products", ***Journal of the American Ceramic Society***, Vol. 82, No. 12, (1999), 3539–3548.
23. Dezhi, Z. and Shuxian, C., "The Effect of Additives on the Properties and Formation of MgO Dense Layer in MgO–C Permeable Samples", ***Proceedings of the Unified International Technical Conference on Refractories***, Kyoto, Japan, 164–70 (1995).
24. Artit, R., Lee, W.E., Argent, B.B. and Larsen, P.H., "Reaction of Aluminum and Silicon in MgO-Graphite Composites and Prediction of Phase constitution using MTDATA", ***High Temperature and Materials Science***, Vol. 3 (1995), 69-103.
25. Brant, P.O.R.C. and Rand, B., "Reactions of Silicon and Aluminum in MgO–Graphite Composites: I—Effects on Porosity and Microstructure", ***Proceedings of the Unified International Technical Conference on Refractories***, (1991), 172–174.
26. Lou, V.L.; Mitchell, T.E. and Heuer, A.H., "Graphical Displays of the Thermodynamics of High-Temperature Gas–Solid Reactions and their Application to Oxidation of Metals and Evaporation of Oxides", ***Journal of the American Ceramic Society***, Vol. 68, no. 2, (1985), 49-58.
27. Baker, B.H. and Brezny, B., ‘‘Dense Zone Formation in Magnesia–Graphite Refractories’’, ***Proceedings of the Unified International Technical Conference on Refractories***, (1991), 168–71.
28. Jitsumori, Y., Yoshida, T. and Yamaguchi, A., "Effect of Starting Materials Characteristics on Microstructures and Properties of Magnesia Carbon Refractories," ***Proceedings of the Unified International Technical Conference on Refractories***, Kyoto, Japan, (1995),140–147.
29. Wang T. and Yamaguchi, A., "Oxidation Protection of MgO–C Refractories by Means of Al8B4C7", ***Journal of the American Ceramic Society***, Vol. 84, No. 3, (2001), 577-582.
30. Yamaguchi, A., "Effects of Oxygen and Nitrogen Partial Pressure on Stability of Metal, Carbide, Nitride, and Oxide in Carbon-Containing Refractories", ***Taikabutsu Overseas***, Vol. 7, No. 1, (1987),] 4–13.
31. S.C. Carniglia, "Limitation on Internal Oxidation-Reduction Reaction in BOF Refractories", ***American Ceramic Society Bulletin***, Vol. 52, No. 2, (1973), 160-65.
32. Tabata, K., Nishio, H. and Itoh, K., "A study on Oxidation-Reduction Reaction in MgO-C Refractories", ***Taikabutsu Overseas***, Vol. 8, No. 4, (1988), 3-10.
33. Sadrnezhaad, S.K., Gharavi, A. and Namazi, A., "Software for Kinetic Process Simulation", ***International Journal of Engineering' Transactions A: Basics***, Vol. 16, No. 1, (2003) 61-72.
34. Mazet, N. and Spinner, B. "Modeling of gas-solid reactions 2. Porous solids", ***International Chemical Engineering,*** Vol. 32, No. 2, (1992), 271-284.
35. Levenspiel, O., "Chemical Reaction Engineering", 3nd Ed., John Wiley, New York, NY, (1999).
36. Ichikawa, K., Nishio H. and Hoshiyama, Y. "Oxidation Test of MgO-C Bricks" ***Taikabutsu Overseas***, Vol. 14, No. 1, (1994), 13-19.
37. Doughty, G. R. and Tovey, L. S., "A Comparison of the Oxidation Behavior in Air at 1050ºC of Natural Flake Graphites." ***Proceeding of the Unified International Technical Conference on Refractories*** H., Sao Paulo, Brazil; (19993), 830-839.
38. Zumdahl, S. S., Chemistry, 3rd edition, D. C. Heath and Company, Lexington, MA, (1993).
39. Teng, F.Y., Ting, J.M., Sharma S.P. and. Liao, K.H, “Growth of CNTs on Fe–Si Catalyst Prepared on Si and Al Coated Si Substrates”, ***Nanotechnology*** Vol. 19 (2008), 095607.
40. CRC. "Hand Book of Chemistry and Physics” 52nd, (1971-1972).
41. Ahmadi, H. R. Sadrnezhaad, S.K., Ne’mati Z., R. Yazdani, Aghaii A. and Paaydar, “Effect of Ferrosilicon-Aluminum Antioxidants on Properties of Magnesia-Graphite Refractories Containing 15 Percent Remained Graphite”, ***Steel Symposium 81st***, Isfahan,, (2002), 610-620 (in Persian).
42. Ghosh, N.K., Jagannathan, P.K., Ghosh, D.N., "Oxidation of Magnesia-Carbon Refractories with Addition of Aluminium and Silicon in Air" ***Interceram***, Vol. 50, No. 11, (2001), 196-202.
43. Smith, J. D., "Reaction Chemistry and Thermochemistry of Magnesia-Graphite Systems Containing Antioxidants" Ph.D. Thesis, University of Missouri-Rolla, (1993).
44. Shouxin, T., Zhaoyou, C., "The Mechanism of Silicon and Silicon Carbide Making Carbon Containing Materials Antioxidizer" ***China’s Refractories***, Vol. 5, No. 4 (1996).
45. Nemati, Z.A., Sadrnezhaad S.K. and Ahmadi Moghari, H.R., "Effect of Ferrosilicon, Silicon and Aluminum Antioxidants on Microstructure and Mechanical Properties of Magnesia-Graphite Refractory" ***Refractories Applications and News***, Vol. 10, (2005) 2-9.
46. Hongxia L., "Synthesis of New Composite Anti-Oxidants and Their Application to Carbon Containing Refractories" ***China’s Refractories***, Vol. 9, No. 2, (2000), 3-6.
47. Benhui, O., Ruikum, W., Zhongxian, W., "The Effects of Non-Metal Additives on Hydratin Resisance of MgO-C Bricks" ***China’s Refractories***, Vol. 9, No. 1, (2000) 29-31.